

A NUMERICAL MODEL FOR THE PREDICTION OF THE INDUCED FLOW IN PULSE JET EJECTOR WITH EXPERIMENTAL VERIFICATION

E.M. Marzouk, A.F. Abdel Wahab, M.A. Awwad, A.I. AbdeZjattah ¹.

Mechanical Engineering Department, Faculty of Engineering
Alexandria University Alexandria 21544, Egypt

ABSTRACT

Unsteady pulsed ejector is based on energy transfer mode that depends on wave action and pressure exchange that become reversible under ideal conditions and therefore, offer higher efficiency and compact design. The lack of fundamental understanding and insufficient analytical tools for design and development presumably appears to have caused of little research work in the area. A numerical model of the pulse ejector is developed to simulate the non-linear wave motion resulting from a pulse generator in both the primary and associated augments tubes. The one-dimensional non-steady conservation equations are solved for variable area geometry with the influence of wall friction, heat transfer and capable to resolve wave formation with flow discontinuities. The developed model is set up with sufficient generality to include all significant processes, which occur in the pulsed ejector. Adequate boundary conditions for the two flow fields and interactions are supplied. An experimental set up is constructed to provide results for comparison with the numerical predictions for steady cyclic operation of the ejector. Excellent agreement is demonstrated between experimental and theoretical results in the pulse frequency range of 50 - 220 Hz and primary stagnation pressures up to 4 bar, based on pressure traces and ratio of secondary to primary mass flow rates. The correlation indicates that the wave events in the ejector are understood in very good detail.

Keywords: Simulation, pulse ejector, performance, Experimental

INTRODUCTION

The pulsed ejectors have been successfully used in pumping and thrust augmentation applications exploiting the unsteady primary flow of the intermittent pulsed type. Pulse ejection action is shown, to be of fundamental importance in the proper design of pressure-gain pulsed combustors for gas turbines and other uses [1-4]. Amongst other pulse jet ejectors applications, include the so called pulsed converters that combine tuned exhaust systems with substantially steady, full admission flow, through turbines turbochargers [5, 6].

Mass and thrust augmentation in pulse ejector systems are produced by virtue of the increased final mass as a result of the entrained surrounding gas. They are reported to have very high performance

levels associated with compact dimensions when compared to steady flow ejectors [7-10]. This higher performance is attributed to the uniqueness of the energy transfer type which depends on wave action and pressure exchange phenomena that become reversible under ideal conditions and therefore offer higher efficiency. This is unlike the steady flow ejectors where the secondary flow is induced through viscous and turbulent mixing [11-13].

In the previous works [7-14], various attempts have been made to separately study the flow phenomena within the pulsed ejector either experimentally or theoretically but not simultaneously. This resulted in the absence of a real theoretical model that possesses the capacity to adequately describe all the flow processes within the ejector ducts. An attempt has

been made by Johnson [15] to conduct a theoretical and experimental study of the pulsed ejector. However, the study employed most rudimentary model that failed to describe certain crucial phenomena within the ejector flow. Marzouk and Mousa [16] reported a theoretical and experimental study but the model did not describe the processes in the augmenter and the flow was assumed to be homentropic.

The present work describes and presents a comprehensive study of the induced flow and thorough numerical model for the whole pulse jet ejector based on the method of characteristics [17 -20]. The developed model is set up with sufficient generality to include all significant processes which occur in the ejector. The convergence of the numerical solution to a condition representing steady cyclic operation is demonstrated. A prototype pulsed ejector is also constructed, thereby offering a means to verify the proposed model. The results of both the experimental and the numerical model are compared from the point of view of mass flow rate ratio and the instantaneous pressure history on both the augmenter and primary tubes.

PRINCIPLE OF OPERATION

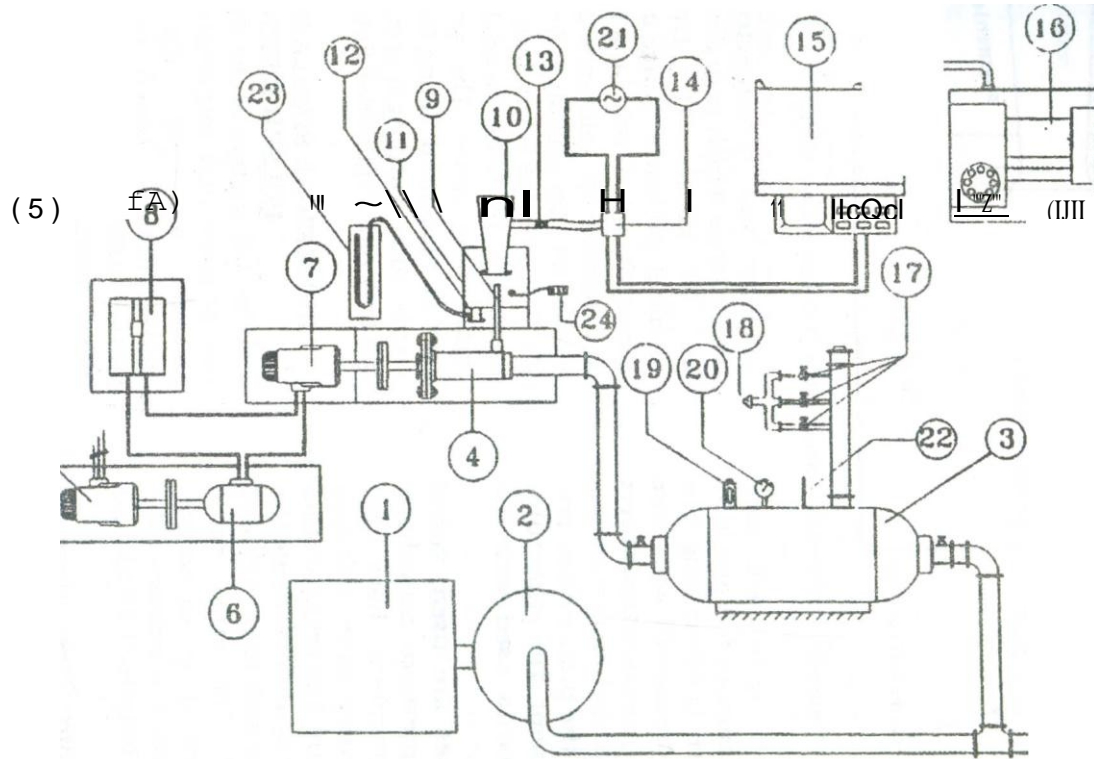
The non-steady operation of the pulsed ejector is essentially a consequence of the pulsed intermittent primary flow generated in an unsteady flow device such as pulsed combustor [2,4], pulsed converter [5,6]. etc. Such intermittent primary flow, upon leaving the primary device, floods the ejector's augmenter tube inlet, thereby generating strong pressure waves that travel to the downstream end of the augmenter where they reflect as rarefaction waves and travel back to the augmenter inlet inducing secondary flow. This secondary flow along with the entrained flow that enters with the primary pulse jet constitutes the augmenting mass that increases the primary mass flow rate and thrust. This secondary flow pertains until another primary pulse strikes the

augmenter inlet and the process is repeated in a cyclic manner. The advantages of the pulsed ejector in terms of mass and thrust augmenting capacity over the steady flow counterpart lies in the dependence of the former on wa~'~ action that necessitates compact configurations for efficient operation. On the other hand, the steady flow ejectors depend on turbulent and viscous mixing between the primary flow and surrounding gas and, therefore, require large configurations for sufficient mixing. This means that pulsed ejector offers lighter and smaller structures making it exceptionally suitable for propulsion applications.

EXPERIMENTAL SET UP

The entire rig assembly is shown in Figure 1 and the prototype pulsed ejector is shown schematic ally in Figure 2. It comprises a pulsating flow generator that produces an intermittent flow in the primary tube. The primary tube exit port and augmenter inlet port are sealed within a large enclosure from which secondary flow could be drawn through the augmenter. This enclosure is equipped with an BS standard flow nozzle [21], such that the secondary flow rate could be determined. The augmenter tube is mounted to the flow box through a threaded flange to allow the variation of augmenter's location. All augmenters are incorporated with a rounded entrance to reduce separation and minimize spill over.

The pulse frequency of the primary flow is varied by changing the pulse generator speed Figure 2, which rotates by a variable speed motor Figure 1. The high pressure air(stagnation pressure) is supplied to the test rig by a 63 kW screw compressor rated at 8.2 mo/min. and 10 bars. The compressor delivers dry air to its 3 m³ pressure vessel which in tum supply the air to a supply tank of 0.5 m³ volume. The stagnation pressure of the primary flow is adjusted at the supply tank via its bleeding nozzle and valves, (see Figure 1).



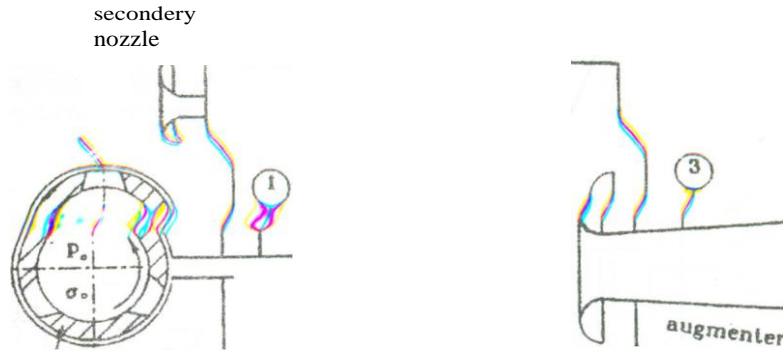
1 Screw compressor. 2
Storage tank.
3 Supply air tank.
4 "P" flow generator. 5
3 phase induction motor. 6
D.C. generator.
7 D.C. motor.

8 Variable resistance.
Primary tube.
9 Accelerator tube. 10
Flow box.
11 Nonle flow meter.
12 Strain gauge pressure transducer. 13
AC-DC adapter & transducer
wired connection.

14 Digital oscilloscope. 15
H.P. oiler.
16 Bleedline valve. 17
Safety valve. 18
Pressure gauge. 19
Single phase AC
supply.

20 Mercury thermometer 21
Inclined U tube manometer 22
Digital thermometer

Figure 1 Schematic diagram of the experimental setup



2

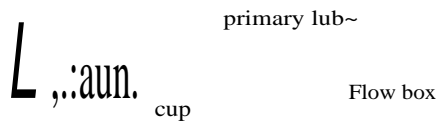


Figure 2 Schematic Diagram of a Prototype pulsed Ejector

Two primary tubes are used, each having 8 mm inside diameter but one is 40 cm long and the other is 48 cm long. The shorter tube is incorporated with two pressure taps for the pressure transducer mounting to pick up the instantaneous pressure signals from the primary flow and discharges to the ambient. The other tube, with no pressure taps, is used with the entire ejector assembly.

Six augmeter tubes are used, two of which have taps for pressure transducer mounting. Three augmeters have inlet areas 4 times the primary tube exit area and are 24 cm in length. The cross section area of one augmeter is uniform while the other two are divergent with total included angles of 3° and 60°. The other three augmeters are uniform in cross section and have ratio of inlet area to primary tube exit area of 12.5 but at lengths 9, 15 and 20 cm.

The calibrated strain gage pressure transducer, type P4VK, has a built-in

amplifier and is connected to an HP digital oscilloscope which is in direct interface with an HP plotter. The transducer has a nominal pressure range of 5 bars, nominal sensitivity of 5 volt at a nominal pressure and sensitivity tolerance ~ ± 0.3 %, with a maximum measurable frequency of 2000 Hz. The average secondary mass flow rate is measured by water head differential across nozzle flow meter. The primary mass flow rate is measured using the same standard nozzle after turning it around and blocking the flow box augmeter flow hole.

NUMERICAL SIMULATION OF THE PULSED EJECTOR

The calculation of the fluid properties in the primary and augmeter flow fields is carried out by the method of characteristics, based on the following partial differential equations representing mass, momentum and energy conservation in one dimension space and in vector notation:

$$\frac{\partial}{\partial t} \begin{Bmatrix} \rho u \\ \rho \left(e + \frac{u^2}{2} \right) \end{Bmatrix} + \frac{\partial}{\partial x} \begin{Bmatrix} \rho u^2 + p \\ \rho u \left(e + \frac{u^2}{2} + p \right) \end{Bmatrix} = \begin{Bmatrix} - \frac{1}{Ar} \frac{dAr}{dx} \\ - \frac{1}{Ar} \left\{ \rho u \left(e + \frac{u^2}{2} + p \right) \right\} \frac{dAr}{dx} \end{Bmatrix} \quad (1)$$

A Numerical Model for the Prediction of the Induced Flow in Pulse Jet Ejector With Experimental Verification

where $G = \frac{\rho u |u|}{2d} \sim \xi$ (2)

represents the friction force per unit mass with friction coefficient f assumed to be that of quasi-steady turbulent flow [22]. The term q represents the heat transfer per unit mass per unit time :

$$q = \frac{4hf}{pD} (T_w - T) \quad (3)$$

he is the film heat transfer coefficient calculated from Reynolds-Colburn analogy [22] and T_w is the wall temperature. Manipulation of the above system of Equations 1, it is transformed into its characteristic form [17, 18]. Non dimensionalization of the equations and using the dependent variables P , U and G , the ordinary differential equations are integrated along their relevant characteristics [17-19]:

$$\frac{-(crB + crN)PB + U_B}{2} = \frac{-(crB + crN)PN + U_N}{2} + \frac{(Y-1)D'' - F''}{Y} \quad NB$$

$$\dots; \frac{(P_0 U) dAr''}{NB dX}$$

6. (4)

Along ($U'' + A''$) characteristics

$$\frac{1}{2} (GB + aM)P_B + U_B = \frac{1}{2} (aB + aN)P_N + U_M$$

$$+ \frac{(Y-1)D'' + F''}{Y} \frac{AZ}{ME} \frac{dAr''}{dX} \quad (5)$$

Along ($U'' - A''$) characteristics

$$aB - a_N = \frac{1}{2} (aB + a_N) \frac{P_B - P_N}{P} \quad (6)$$

Along particle path U'' characteristic

$$D'' = \frac{(y-1)}{2} \frac{(q'' + U''G^*)}{A''}$$

$$H'' = \frac{J}{2} \frac{Y-1}{A''} \sim (q'' + U''G^*) - 1$$

$$F'' = \frac{v}{2} G^*$$

The above equations are solved algebraically to find the values of the dependent at the new time level for internal nodes, Figure 3. The double subscripts denote average quantities over the relevant characteristic, Rather than taking the weighted averages of the relevant characteristic slopes on both sides of each point, (N,M,J of Figure 3) [18], and then linearly interpolate for the dependent variables. The present technique preserve the physical interpretive quality of the numerical representation of the characteristics. Thus, reference to Figure 3,

the technique presented for subsonic flow as:

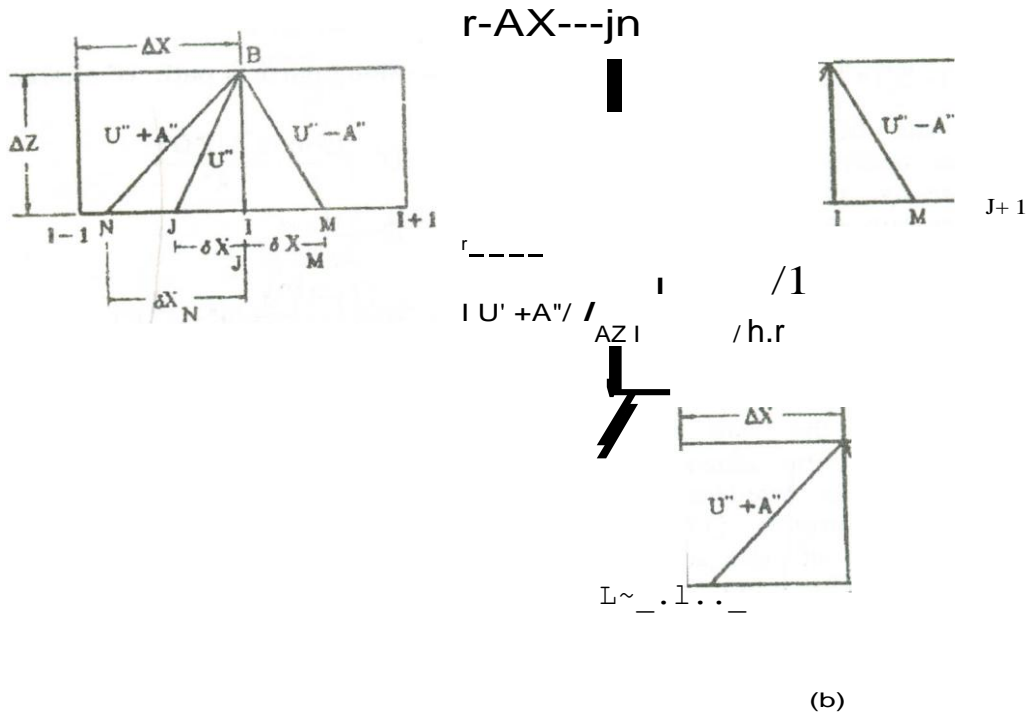
$$Y = \frac{U_I + P_I cr_I}{2}$$

$$[\dots; \frac{1}{2} (U_r + P_r) - \frac{1}{2} (U_{I-1} + P_{I-1})] \quad (7)$$

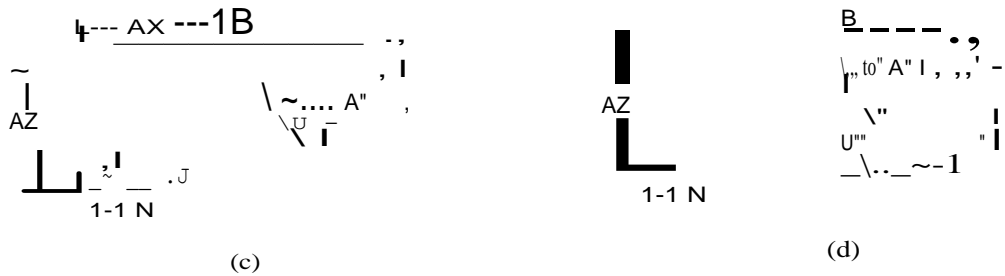
$$\left(\frac{\delta X}{\Delta X} \right)_N - \frac{\delta X}{\delta CM} \text{ and } (\sim) \text{ are also developed, } \frac{\delta X}{\delta XJ}$$

Linear interpolation of the dependent variables is:

$$P_{N,M,J} = P_I - \left(\frac{P_I - P_{I-1}}{X_I - X_{I-1}} \right) (X_N - X_{I-1}) \quad (8)$$



(8)



(c)

(d)

Figure 3 Glid System and Characteliisics for the modified method of characteristics for subsonic flow (——— Real; - - - - - Non-existent; (a) Internal Grid; (b) Left Hand Boundry, Inflow; (c) Right Hand Boundary, Outflow; (d) Right Hand Boundary, Inflow).

The missing information required to obtain the dependent variables at the boundary node points of the flow fields Figure 3, are obtained through the boundary conditions by application of the conservation equations of mass and energy in quasi-steady forms[17,20]. The flow information of the primary flow as it enters the augmenter duct is numerically supplied through mass, momentum and energy balance technique at any instant. The technique, developed in one dimensional space, is devised due to the meager analytical and experimental knowledge of the intermittent primary jet as it enters the augmenter tube. The resulted equation of the technique in non dimensional form is :

$$\dot{M}_2^2 P_{o_2}^2 \sigma_{o_2}^2 + \dot{M}_1 (P_{o_1}^2 \sigma_{o_1}^2 + P_{o_2}^2 \sigma_{o_2}^2) \dot{M}_2 + \dot{M}_1^2 A_1^2 (I - Ar) = 0 \quad (9)$$

This quadratic equation in M_2 determines the amount of entrained fur entering during the primary flow period at each time step. Once M_2 resolved, then Ma , U_a and θ_a are determined and used as boundary condition for augmenter inlet port. Full details of the numerical simulation procedure is available [20].

ANALYSIS OF CALCULATED AND EXPERIMENTAL RESULTS

Figures 4 and 5 present a comparison between the pressure time history obtained experimentally and numerically for the primary tube. As the pulse generator rotating cup opens, compression waves travel to the open end of the primary tube which accounts for the initial pressure rise at the beginning of the cycle. These waves reflect back at the primary tube exit as expansion waves which enhance outflow from the tu be.

A Numerical Model for the Prediction of the Induced Flow in Pulse Jet Ejector With Experimental Verification

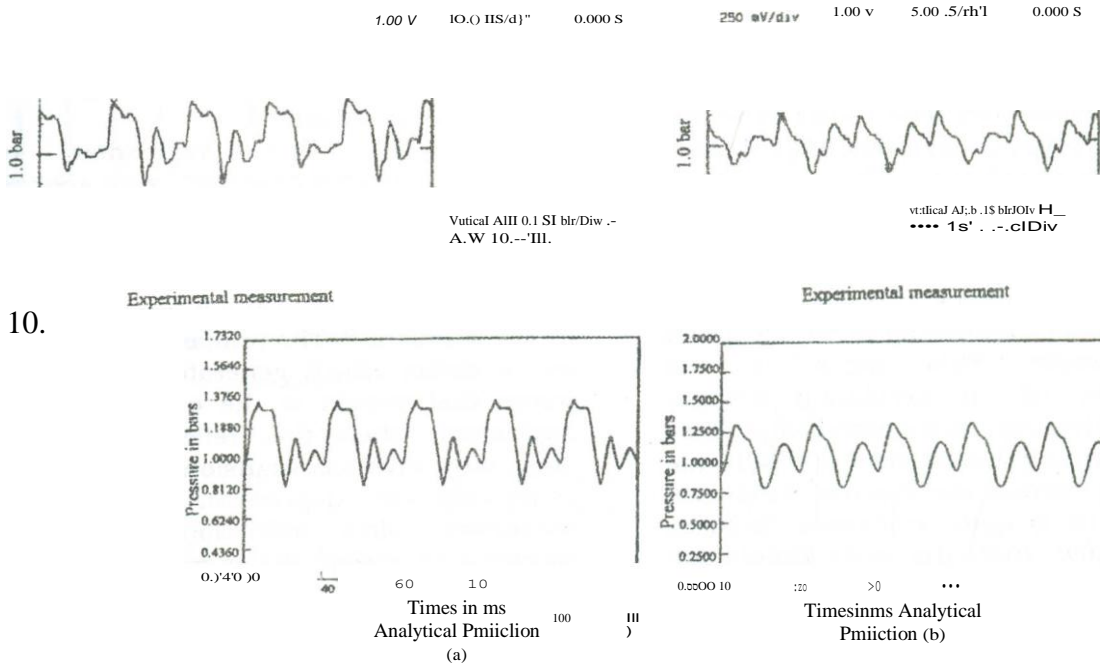


Figure 4 Pressure Time History Recorded from the primary tube ((a) at Station 2, 2.5 bars stagnation pressure, 298K stagnation Temperature and 1000 rpm Motor Speed, (b) at Station 1, 1.5 bars Stagnation pressure, 298 K Stagnation Temperature and 2000 rpm Motor Speed).

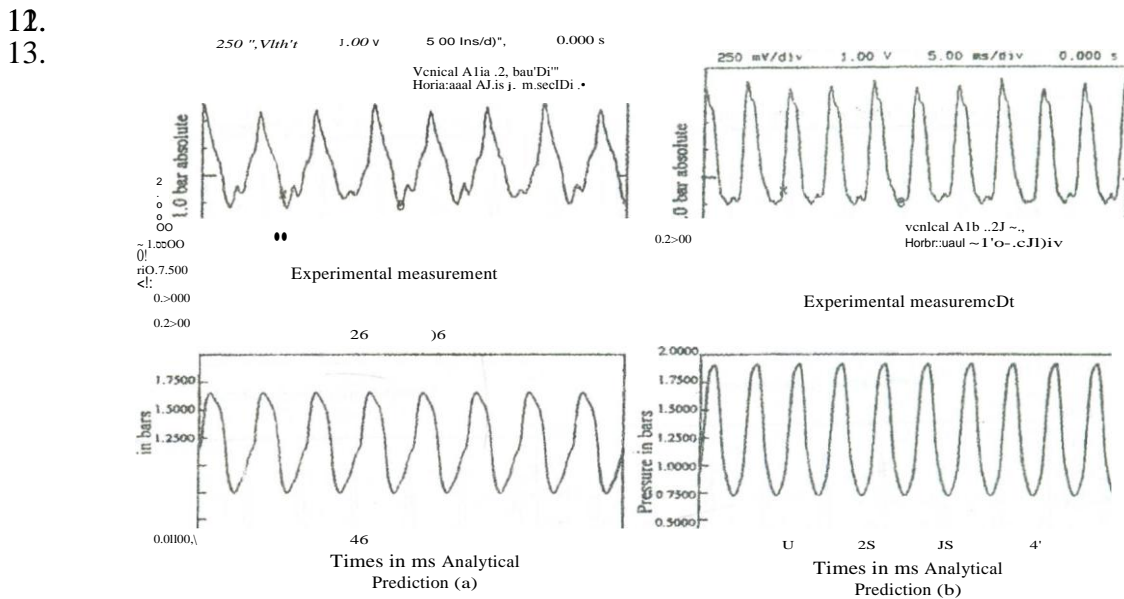


Figure 5 Pressure-Time history recorded from the primary Tube ((a) at station 2, 2.0 bars stagnation pressure, 298K stagnation temperature and 3000 rpm Motor Speed, (b) at Station 1, 1.5 bars stagnation pressure, 298 K stagnation temperature and 4000 rpm motor speed)

At low pulse frequency, the expansion waves have ample time to reflect at the open end of the tube and travel back to the currently closed inlet where they reflect once more and the process continues in a repetitive manner until the port opens again. This accounts for the rapid pressure rises and pressure falls during each cycle at low pulse frequencies. At high frequencies, however, by the time the expansion waves travel back to the tube inlet the port will be reopening to initiate a new pressure cycle. This leads to the disappearance of the oscillating pressure traces and the pressure cycles comprise only substantial pressure rises and falls due to inlet port opening and closure. As shown, the agreement is quite evident; sufficiently close to show that the wave events are identified with all its detailed feature. The maximum deviation between the numerical and experimental reading is determined as 5.2%. The small pressure spikes in the experimental recordings appear to be due to small eccentricity of the rotary cup which leads to sudden partial opening and closure of the port during its supposed closure. The

build up to shock waves with excessive rate of pressure rise from the generated pressure waves by increasing the cup speed, is also observed.

The augmeter results of the experimental and analytical pressure-time traces are shown in Figures 6 and 7. The flow phenomena in the augmeter indicates that the primary jet strikes the augmeter as a slug at different entropy level from the flow in the augmeter. The primary jet, thus, acts as a piston which generates compression waves that travels to the other end of the augmeter where they reflect back to the augmeter inlet as expansion waves ,thereby generating the depression responsible for secondary flow induction. The waves continue to sweep the augmeter back and forth until another primary jet enters the augmeter . This accounts for the rapid rises and falls during each cycle. The maximum percent deviation between the results is determined as 7%. This deviation is attributed to errors originated from the numerical approximations as well as from uncertainties of experimental recordings.

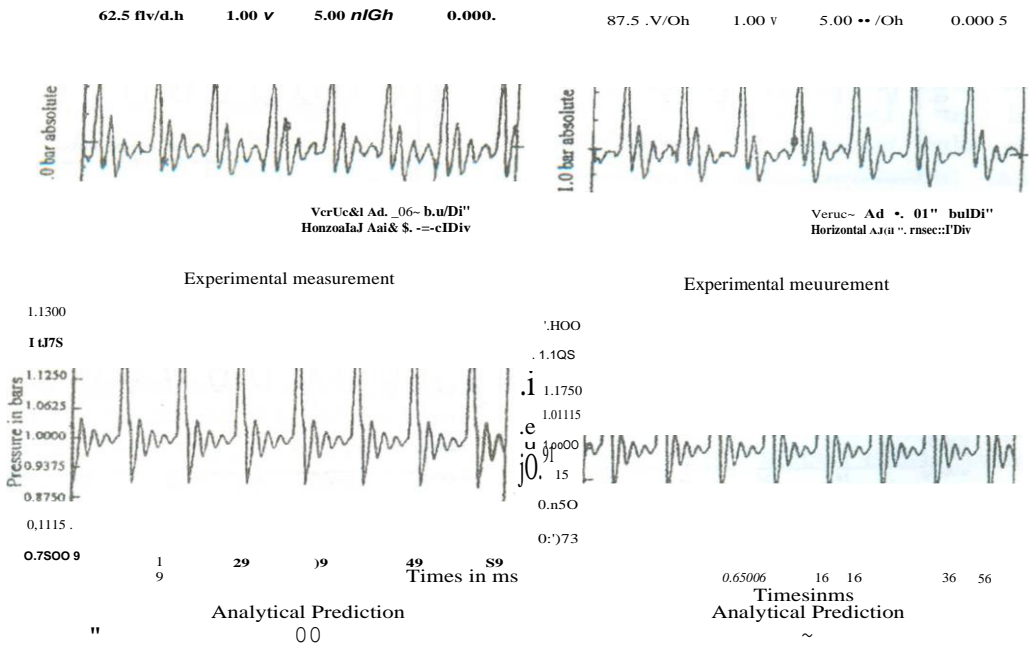


Figure 6 Pressure Time History recorded from the augmeter tube (a) at station 3, 2.0 bars stagnation pressure, 298K stagnation temperature, 3000 rpm motor speed and 30 degree divergence angle; (b) at station 3, 2.5 bars stagnation pressure, 298 K stagnation temperature, 3000 rpm motor speed and 30 degree Divergence Angle

A Numerical Model for the Prediction of the Induced Flow in Pulse Jet Ejector With Experimental Verification

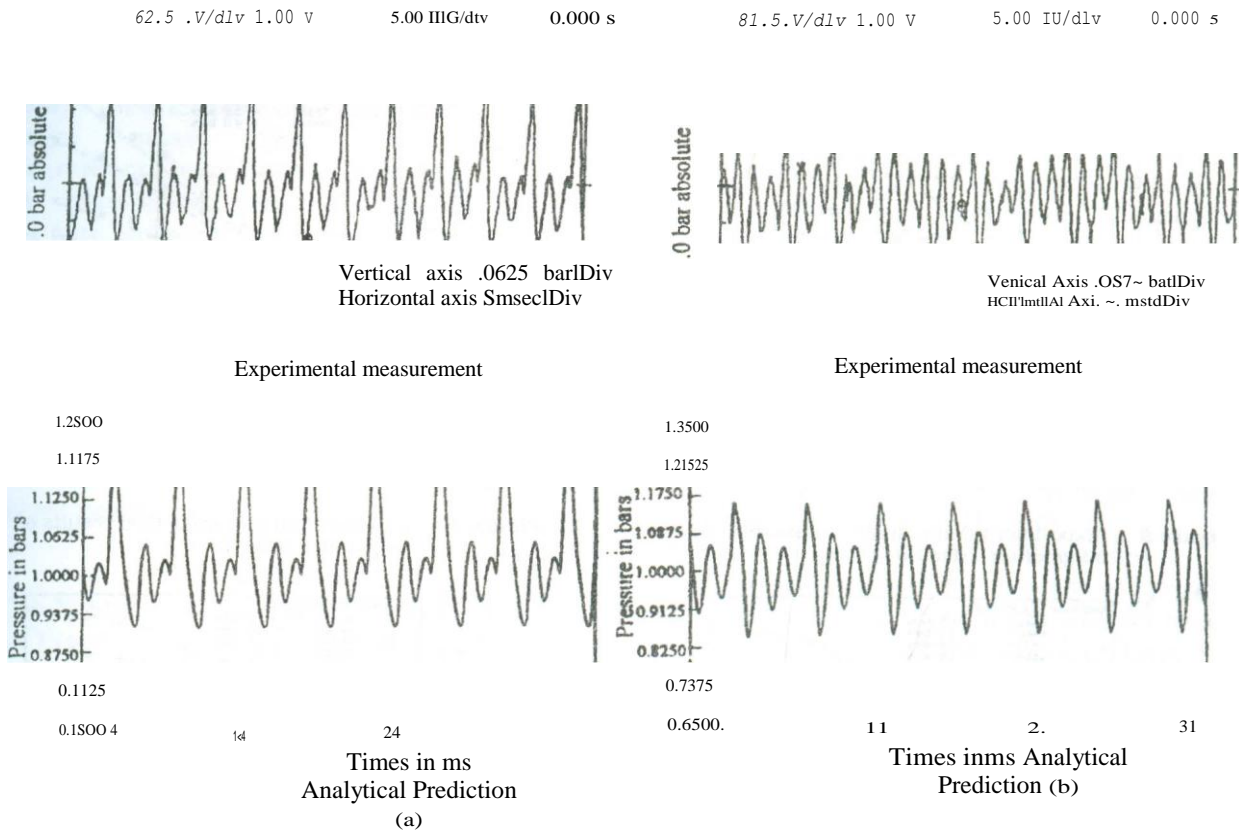


Figure 7 Pressure Time History recorded from the augmentor tube. ((a) at station 3, 2.0 bars stagnation pressure, 298k stagnation temperature, 4400 rpm motor speed and 0° divergence angle (b) at station 3, 2.5 bars stagnation pressure, 298 k stagnation temperature, 4400 rpm motor speed and 6° divergence angle

The overall implication in comparison of results of both the primary and augmentor tubes, reveals that the numerical model generates a wave mechanism identical to actual wave mechanism. The very close correlation indicates that the wave events in the pulse jet ejector are understood in very good detail. Figures (8-13) show the experimentally measured and corresponding analytical predictions of mass flow rate ratio, as a function of frequency for different primary stagnation pressures. The results correlate favorably with a maximum between theoretical and experimental results of 3.1 %. All data show a rising characteristic as the frequency increases due to the increased momentum of the primary jet and hence the augmentor

secondary flow. However, the mass flow ratio of the ejector decreases as the primary flow stagnation pressure increases. This is due to the increased entropy discontinuity with which the primary flow enters the augmentor. The rarefaction waves, then, weaken upon colliding with this contact discontinuity and hence the depression at the augmentor inlet does not increase the secondary flow with the same proportion as the primary flow. The increase of the augmentor divergence angle is shown to enhance the secondary flow due to the increased depression at the augmentor inlet which results from the wave interaction with the diffusing area change.

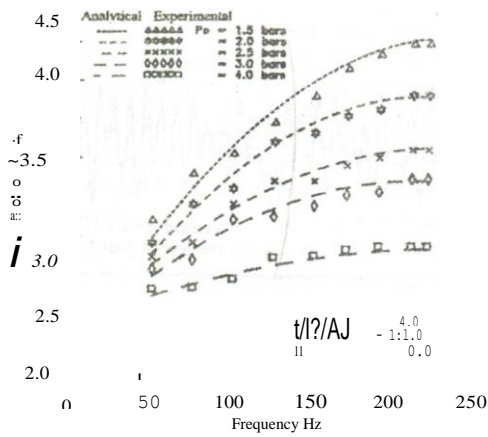


Figure 8 Experimental and analytical results of Augmenter Tube No. 1

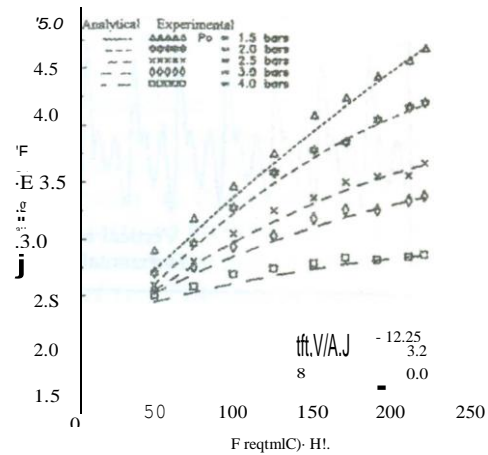


Figure 11 Experimental and analytical results of Augmenter tube No. 4

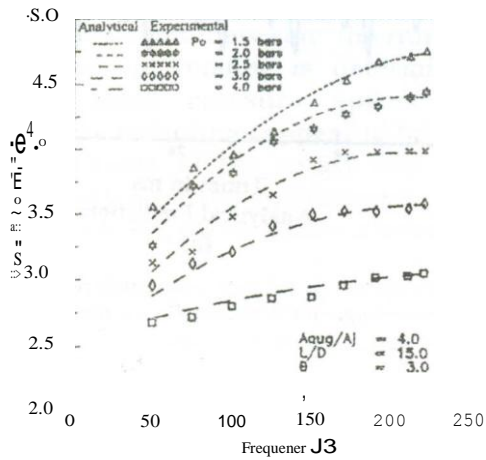


Figure 9 Experimental and analytical results of Augmenter tube No. 2

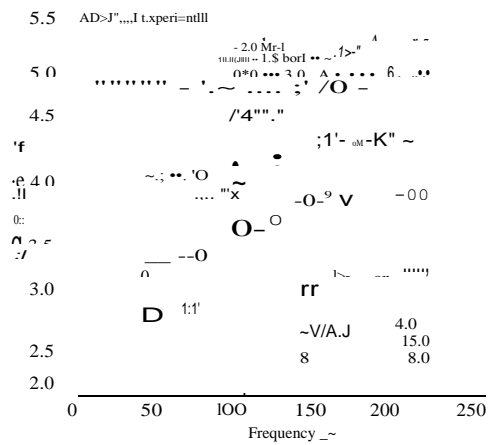


Figure 12 Expelmental and analytical results of Augmenter tube No. 5

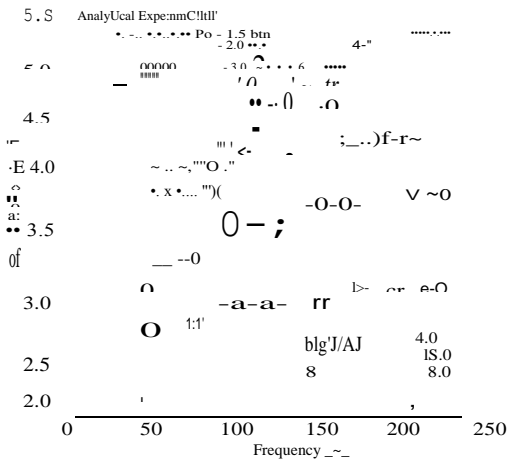


Figure 10 Experimental and analytical results of Augmenter tube No. 3

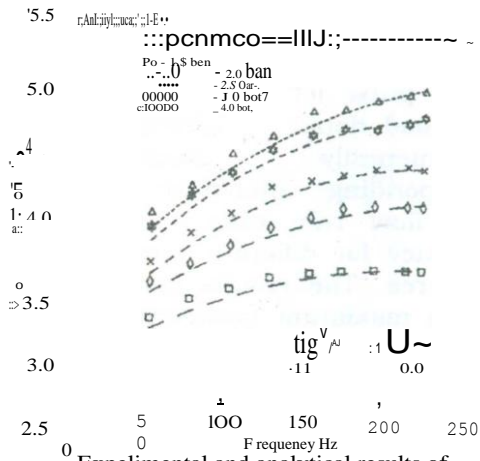


Figure 13 Experimental and analytical results of Augmenter tube No. 6

CONCLUSIONS

On a special test rig, which simulates the non-steady flow in the pulsed ejector system, instantaneous pressures and average mass flow rate ratios measurements have been carried out.

A simulation numerical model that takes into account all intrinsic features of the pulsed ejector flow phenomena, is developed. The very close correlation between experimental and theoretical predictions indicates that the wave events in the ejector are understood in good detail. The results of the model and experimental measurements are in good agreement and can, therefore, be used to optimize the ejector geometry.

REFERENCES

1. E.S. Marzouk, and J.A.C. Kentfield, "Pressure- Gain Combustion a Means of Improving the Efficiency of Thermal Plant," Proceedings 9th Intersociety Energy Conversion Engineering Conference, (Published by American Society of Mechanical Engineers), San Francisco, pp. 1125 - 1131, (1974)
2. J.A.C. Kentfield, M. Rehman, and E.S. Marzouk, "A Simple Pressure Gain Combustor For Gas Turbines", Paper No. 76- GT- 6, pp 1-6. (1976). Transactions of ASME, Journal of Engineering For Power, also ASME, vol.99 No.2, pp. 153-158, (1977).
16. J.A.C Kentfield, and M.J. O-Blenes, "Application of a Second Generation Pulse, Pressure-Gain, Combustor to a Small Gas Turbine", AIAA Paper AIAA87-2156 (Also AIAA J. of Propulsion, Vol. 6, No. 2, pp. 214-220, (1990).
17. J.A.C. Kentfield, and L.C.V. Fernandes, "Further Developments of an Improved Pulse, Pressure Gain, Gas Turbine Combustor" ASME Proceedings of the Aero engine Congress and Exposition. Brussels, Belgium June Paper No. 90GT-84 pp. 1-6, (1990)
18. N. S. Jonata, and N. Watson, "Pulse Converters, A Method of Improving the Performance of Turbocharged Diesel Engine", Proceedings of the Institute of Mech. Engineers, VoL 187, No 51/73, pp. 635-647, (1973).
6. D.E. Winterbone, J.R. Nichols, G.!. Alexander, and S.K. Sinha, "The Evaluation of the Performance of Exhaust Systems Equipped with Integral Pulse Converters "Cimac, Int. Congress on Combustion Engines, Oslo, Paper No. 062, (1985).
7. RM. Lockwood, "Interim Summary Report Covering the Period from 1 April to 30 June 1962 on Investigation of the Process of Energy Transfer from an Intermittent Jet to a Secondary Fluid in an Ejector- Type Thrust Augmenter", Hiller Aircraft Corporation Report No. Ard- 305, June 30, (1962).
8. RM. Lockwood, and H.W. Sander "Investigation of the process of Energy Transfer from an Intermittent Jet to a Secondary Fluid in an Ejector Type Thrust Augmenter", Summary RepNo. Apr 64-4, April, (1964).
9. G. Binder, and H. Didelle, "Improvement of Ejector Thrust Augmenting by Pulsating or Flapping Jets; Second Symposium on Jet Pumps and Ejectors and gas Lift Techniques", Cambridge, British Hydrodynamic Research Association. Paper No. E- 2, (1975).
10. J.V. Foa, "Consideration on Steady and Non Steady Flow Ejector", Proc. of Ejector Workshop for Aerospace Applications, Dayton Ohio, pp. 659688, (1981).
11. P.M. Bevilacqua, "Evaluation of Hyper-Mixing Nozzles for Thrust Augmenting Ejectors", AIAA; Journal of Aircraft, VoL11, No. No.6, pp. 348- 354, (1974)
12. W.M. Presz, R. Gousy, and B. Morin, "Forced Mixer Lobes in Ejector Designs", AIAA Paper, pp. 86-1614, June (1986).
13. W.M. Presz, B.L. Morin, and RF. Blinn, "Short Efficient Ejector Systems," AIAA Paper, pp. 87-1837, (1987).
14. J. K. Johnson "An Experimental Investigation of Ejector Performance for non- steady Flow Conditions," Clemson University Experimental Station Bulletin 107, (1966).

15. W.S. Johnson, "Analytical and Experimental Study of the Pulse-Jet Ejector", University Microfilms International. Ph.D. Thesis, (1967).

16. E.M. Marzouk, and M. Mousa, "Theoretical Optimization for Full Potential of Unsteady Fluid Flow Ejector", Bulletin of Fac. of Eng., Vol. XXII, (1983).

17. E. Jenny, "Unidimensional Transient Flow With Consideration of Friction, Heat Transfer and Change of Section," The Brown Boven Review, pp. 447- 461, (1950)

18. D.B. Spalding and R. Issa "Unsteady Compressible Frictional Flow with Heat Transfer," J. Mech. Eng. Sci, Vol. 14. No. 6, pp. 365-369, (1974).

19. E.M. Marzouk, A.F. Awwad and F. A. Abdel Wahab, "A Comparative Study of Some Finite Difference Schemes in an Unsteady Discontinuous Compressible Flow Field," Bulletin of Fac. of Eng., Vol. 33, No. 3, pp. 151-161, (1994).

20. A.F. Abdel Wahab, "Performance and Optimization of Non-Steady Pulsed Ejector with Experimental Verification", M.Sc. Thesis, Mechanical Eng. Dept., Alexandria University, (1996).

21. "British Standard Institution. Methods of Measurements of Fluid Flow in Closed Conduits", BS 1042: Section 1.1, (1981).

22. J.P. Holman, Heat Transfer, 6th ed., McGraw- Hill, Ny. (1986).

Received September 30, 1998
Accepted February 6, 1999

NOMENCLATURE

Symbol & Unit	Non dimensional Form	Meaning
a (m/s)	$A = a/a_{ref}$	Sonic Speed
A_r (m ²)	$A_r = A_r / A_{ref}$	Duct area
D (m)		Augmenter inlet diameter
e (J/kg) G		Specific internal energy
(N/kg)	$G^* = G \cdot x_{ref} / a^2_{ref}$	Friction force per unit mass
m (kg/s)	$\dot{m} = \frac{\rho \cdot A \cdot a_{ref}}{Pref \cdot Ar_{ref}}$	Mass flow rate
p (Pa.)	$P = \frac{P}{Pref}$	Pressure
q (J/kg s)	$q = \frac{q_{x_{ref}}}{a_{ref}}$	Heat transfer per unit mass
R		Gas Constant
s (J/kg'K)	$\sigma = c_p \left(\frac{\gamma - 1}{\gamma} \right)^{1/\gamma} / R$	Entropy
t (sec)	$Z = \frac{t a_{ref}}{x_{ref}}$	Time
T (K)		Static temperature
u (m/s)	$U = \frac{u}{a_{ref}}, U = \frac{U}{a_{ref}}$	Gas velocity
x (m)	$X = x / x_{ref}$	Distance

Greek Symbols γ

(degree)
(kg/m³)

Adiabatic index
Divergence angle
Gas density

Subscripts

Ref,0

Reference conditions and tagnation
conditions

t,p

Superscripts

Total and primary mass flow

" * ,

Non dimensional variable

$$\dots \sim \sim \backslash J \backslash t \sim \backslash 0 \sim y \sim J \sim p \sim \sim \backslash \sim h \backslash 1 \sim \sim j C;$$

< tw \ -\ \sim \ \sim \ C \ tii \ -\ \sim \ J \ j \ .C \ \sim \ J \ y \sim \) \ -\ \sim \ , " , J . J \ j \ \sim \ . J , " , J j y \sim \ \sim \ J . 1 & .. \sim \ \sim \ \sim \ \sim \ (. 5 , ill \sim \ . li A

~

ملخص البحث

~.r:d \ ~ \ .4 ; A . o C J W \ ~) } 2 J) } 2 J . li J . ~ I 04 . ; - 1 j ~ J J \ o ~ 4 j d \ \sim i J \sim \ C J W \sim \ t \sim \ J . > \sim J S . ~ 4) C) j \sim \sim
j : . A \ \sim J J - o I ' y l \sim i j \sim j . ; J . ; J J \sim \sim . } \sim j t k ; . \sim j J . ; . ; \sim \sim I J J \ Y p i ' J ' J \sim \ J \sim L ; J \sim Q \sim " ; ; \sim) j \sim J J y . . > \lambda \sim I \sim I ' i \backslash
04 . ; - 1 ' " S W \ \$ ' , J l > . \sim \sim p \ ; - i J \sim W l j I : ! J \sim J \backslash \dots ; ; L - b U i j . : A 0) y . \backslash J o ' \sim \backslash . r S ^ G , 1 ; ; 4 W " - . > y ; . \sim j J \sim ' i \backslash 04 . -- J I I J . : o !
4 b l . 4 \ ; i j \sim \ C \sim . " . : J I \sim) W \sim \sim r : ' W \ ; -) Y d ' f i \sim \sim j \sim \sim f W " 4 A j \sim . I I \sim \dots ; ; i \sim \sim J . I I J C . ; U \ 04 . ; - 1 j . > i f - l
~) : z . J I \sim \backslash : J \sim

J \sim W ,) \backslash A L . - . \sim I J \sim L A d i " ; ; I . : > ; } I . r . S ^ U J S - \sim \sim \backslash C J W \backslash \sim I \sim i \backslash 04 . -- J \backslash o \sim 4 j 0 i \sim \backslash H i . li J \sim L . d \backslash \sim 4 \sim \sim) . ! 4 A 9 \backslash p r : ' W
J S - J r : J - I f J . 04 . ; - 1 \sim I C J W \backslash J W " C ; U \ . k , l j . \backslash J S - \sim j (\sim L . J - I ! \sim I - . : : J W \backslash J ; " - ' \sim 4 ! : . . J \sim . s J I . ; A l ') a . \backslash \sim J J Q - j
J S - C . . r U ^ l C \sim . " . : J \backslash 4 . . r \sim \sim . > \lambda \backslash f ' J \backslash \sim) : z . J I J \sim \backslash

. \backslash A L . . . \sim I J " ; ; I . : > ; } \backslash 4 ! : . . J I J ; o - \backslash \sim I A J \sim \backslash . i s ' J